journal of the mechanical behavior of biomedical materials 153 (2024) 106470

Contents lists available at ScienceDirect

Journal of the Mechanical Behavior of Biomedical Materials

journal homepage: www.elsevier.com/locate/jmbbm

Mechanical loading of *ex vivo* bovine trabecular bone in 3D printed bioreactor chambers

Brian A. Kunath [a,b,*], Kail Beloglowka [a,b], Roshni Rainbow [a,b], Heidi-Lynn Ploeg [a,b]

[a] Department of Mechanical and Materials Engineering, Queen's University, Kingston, ON, Canada
[b] Centre for Health Innovation, Queen's University, Kingston, ON, Canada

ARTICLE INFO

Keywords:
3D printing
Bioreactor
Bone mechanics
MED610^{TM}
Trabecular bone organ culture

ABSTRACT

Previous *ex vivo* bone culture methods have successfully implemented polycarbonate (PC) bioreactors to investigate bone adaptation to mechanical load; however, they are difficult to fabricate and have been limited to a 5 mm maximum specimen height. The objective of this study was to validate a custom-made 3D printed MED610^{TM} bioreactor system that addresses the limitations of the PC bioreactor and assess its efficacy in *ex vivo* bone culture. Twenty-three viable trabecular bone cores (10 mm height by 10 mm diameter) from an 18-month-old bovine sternum were cultured in MED610^{TM} bioreactors with culture medium at 37 °C and 5% CO_2 for 21-days. Bone cores were ranked based on their day 0 apparent elastic modulus (E_{app}) and evenly separated into a "Load" group (n = 12) and a control group (n = 11). The Load group was loaded five times per week with a sinusoidal strain waveform between −1000 and −5000 με for 120 cycles at 2 Hz. E_{app} was assessed on day 0, 8, and 21 using quasi-static tests with a −4000 με applied strain. Over 21-days, the E_{app} of Load group samples tended to increase by more than double the control group (53.4% versus 20.9%) and no visual culture contamination was observed. This study demonstrated that bone organ culture in 3D printed MED610^{TM} bioreactors replicated E_{app} trends found in previous studies with PC bioreactors. However, further studies are warranted with a larger sample size to increase statistical power and histology to assess cell viability and bone mineral apposition rate.

1. Introduction

In Canada, 10% of adults over the age of 40 and 21% of post-menopausal women are estimated to suffer from osteoporosis (Kendler et al., 2021). Osteoporosis is a skeletal disease characterized by low bone mineral density and the deterioration of bone tissue, leading to increased bone fragility and chance of fracture (Clynes et al., 2020; Kendler et al., 2021). Between 2015 and 2016, over 2.2 million osteoporosis diagnoses were made in Canada, with over 130,000 fracture patients, contributing to an annual economic cost of $4.6 billion (Canadian Chronic Disease Surveillance System, 2021). Fragility fractures in men and women over the age of 50 are projected to increase by an average of 24% across Canada by the year 2030 (Kendler et al., 2021). Hip fractures are recorded to be the most fatal osteoporotic fracture type, with 12-month post-fracture mortality rates as high as 22% and 33% for women and men, respectively (Kendler et al., 2021).

Further insights into bone biomechanics could lead to the advancement of bone fracture prevention and treatments for bone diseases and injuries, such as osteoporosis (Little-Letsinger et al., 2022; McMillan et al., 2017; Tong et al., 2019). Mechanical stimulation is one of several factors understood to promote bone modelling and remodelling (Currey, 2012; Frost, 2003; Martin et al., 1998). Bone tissue response is dependent on the applied magnitude and rate of strain (Frost, 1987; Ozcivici et al., 2010). Below strains of 100 με bone resorption occurs, while strains between 1000 and 3000 με are theorized to promote bone adaptation (Frost, 1987, 2003). Above these strains, bone is susceptible to microdamage with fracture likely around 25,000 με. However, these ranges are approximations and exact thresholds are likely dependent on multiple factors (anatomical location, species, bone volume fraction and more) and yet to be identified (Rosa et al., 2015).

Bone response to mechanical stimulation can be evaluated using various techniques with *in vivo* or *ex vivo* applications (Rosa et al., 2015). *Ex vivo* bone organ culture methods allow for the simplification of *in vivo* complexities (e.g., removal of systemic factors) and the mechanical stimulation of viable bone in long-term culture studies while providing a

* Corresponding author. 130 Stuart Street, Kingston, ON, K7L 2V9, Canada.
E-mail addresses: b.kunath@queensu.ca (B.A. Kunath), 15kb60@queensu.ca (K. Beloglowka), roshni.rainbow@queensu.ca (R. Rainbow), heidi.ploeg@queensu.ca (H.-L. Ploeg).

https://doi.org/10.1016/j.jmbbm.2024.106470
Received 29 October 2023; Received in revised form 5 February 2024; Accepted 16 February 2024
Available online 17 February 2024

List of symbols

2D	Two-dimensional
3D	Three-dimensional
$\%\Delta E_{app}$	Percent change in apparent elastic modulus
AA	Antibiotic-antimycotic
A_c	Cross-sectional area, mm^2
CO_2	Carbon dioxide
D	Bone core diameter, 10 mm
DMEM/F-12	Dulbecco's modified eagle/F-12 ham culture medium
E_{app}	Apparent elastic modulus, MPa
F	Force, N
FBS	Fetal bovine serum
H	Bone core height, 10 mm
NaCl	Sodium chloride
NaOH	Sodium hydroxide
Na_2SiO_3	Sodium metasilicate
PC	Polycarbonate
PGE2	Prostaglandin E2
R^2_{avg}	Average coefficient of determination
SD	Standard deviation
SEM	Standard error of mean
w/v	Weight per volume
α	Statistical level of significance
δ	Displacement, mm
ε	Strain, mm/mm
με	Microstrain

controlled environment that replicates accurate physiological conditions, such as native cell-cell and cell-matrix extracellular matrix interactions (Bellido and Delgado-Calle, 2020; Cramer et al., 2021; Marino et al., 2016; Rosa et al., 2015). Previous *ex vivo* human and bovine trabecular bone studies have successfully implemented a polycarbonate (PC) bioreactor system combined with a mechanical loading system to investigate trabecular bone adaptation in response to mechanical load (Davies et al., 2006; Meyer et al., 2016; Vivanco et al., 2013). Compressive bulk strains between 2000 and 4000 με have been shown to cause an increase in *ex vivo* bovine and human trabecular bone apparent elastic modulus (E_{app}) compared to non-loaded samples (David et al., 2008; Endres et al., 2009; Mann et al., 2006; Meyer et al., 2016; Vivanco et al., 2013).

Despite the PC bioreactor advantages, they are difficult and expensive to manufacture and have been limited to testing cylindrical bone specimens with maximum dimensions of 5 mm × 10 mm (height (H) x diameter (D)). To prevent sample buckling and ensure accurate bone mechanical property measurement, a standard aspect ratio – the ratio of height to diameter – between 1 and 2 is recommended (Zhao et al., 2018). Previous *ex vivo* trabecular bone core studies limited core height to increase diffusion of culture medium nutrients into the core centre (Davies et al., 2006; Meyer et al., 2016; Vivanco et al., 2013). It is not known whether larger cores can be maintained in long-term culture. With the advancing technology of additive manufacturing, 3D printing can reduce fabrication costs and difficulty (Kreβ et al., 2020; Mustahsan et al., 2021; Priyadarshini et al., 2020) and allow for flexible design optimization (Su et al., 2021), high dimensional precision (Heuer et al., 2021), and biocompatible material options (Ngan et al., 2019). To address the limitations of the previous PC bioreactors, a custom-made 3D printable bioreactor using the photopolymer MED610™ has been developed. However, MED610™ biocompatibility in bone organ culture remains unknown. Although MED610™ is classified as a biocompatible material with mucosal membrane contact for up to 24-h (Stratasys, 2018), recent publications suggest that if adequately cleaned, MED610™ is suitable for long-term culture experiments (Currens et al., 2022; Ngan et al., 2019). Therefore, the objective of this study was to test the 3D printed bioreactor system in a long-term *ex vivo* bovine trabecular bone experiment with 10 mm high bone cores. Bioreactor efficacy was assessed by quantifying the bone adaptation response to mechanical loading using the change in E_{app} over 21-days, as implemented by Vivanco et al. (2013). For the purpose of this study, the authors prioritized maintaining tissue viability and E_{app} change over time rather than material characterization.

2. Methods

2.1. *MED610™ part 3D printing and preparation*

Bioreactor chambers were designed in SolidWorks (2019) (SolidWorks Corp., Dassault Systemes, Waltham, MA, USA) and adapted from the Zetos design employed by Vivanco et al. (2013) and Meyer et al. (2016). Bioreactor parts were 3D printed with an Objet30 Prime 3D printer, MED610™, and SUP706B™ support material (Stratasys, Edina, MN, USA). After printing, all visible support material was removed with a pick tool and a high-pressure waterjet bath. Remaining support material was removed in a 1% w/v sodium metasilicate (Na_2SiO_3) and 2% w/v sodium hydroxide (NaOH) solution, following the manufacturer's recommendations (Stratasys, 2018). Parts were then cleaned with a sonication protocol (Ngan et al., 2019) and autoclaved for 4 min at 132 °C. Custom-made MED610™ test tube stoppers for medium reservoirs were cleaned following the same procedure. Detailed mechanical drawings of parts are available from the authors.

2.2. *Preparation of bovine trabecular bone cores*

A bovine sternum (Fig. 1 (A)) was excised from a healthy 18-month-old animal and obtained from a local abattoir. Bone core preparation began within 2 h post-slaughter. Under sterile conditions, the sternum was sectioned at the cartilage intersections using an Exakt 312 diamond-coated pathology saw (Exakt Advanced Technologies, Norderstedt, Germany) with continuous water irrigation. Trabecular bone sections were cut into 12 mm thick slices (Fig. 1 (B)) and then cored into 12 mm × 10 mm (H x D) samples (Fig. 1 (C)) with a custom-made coring bit and a vertical mill (CX605, Busy Bee Tools, Concord, ON, Canada). After coring, bone cores were clamped and milled with a 4-fluted endmill (No. 8918A53, McMaster-Carr, Elmhurst, IL, USA) to obtain a height of 10 mm and ensure samples had flat and parallel surfaces (Fig. 1 (D)). To prevent dehydration between coring and milling, samples were placed in sterile dishes with sterile culture medium: DMEM/F-12 (MilliporeSigma, Burlington, MA, USA), supplemented with 10% fetal bovine serum (FBS, MilliporeSigma) and 5% antibiotic-antimycotic solution (AA, MilliporeSigma). Bone core specimens were submerged and irrigated with sterile 0.9% sodium chloride (NaCl) solution at 4 °C during coring and milling. NaCl solution was aspirated and replaced often to maintain sample visibility. Coring and milling were performed at slow speeds (~300–400 rpm) to prevent bone exposure to significant heat generation and damage. A total of 40 bone cores were obtained and washed in medium. Cores were placed in 24-well plates with medium and incubated at standard culture conditions of 37 °C and 5% CO_2 for 4-days to allow time for recovery. The 4-day recovery period was chosen for practical reasons with the same conditions applied for the experiment. Each bone core height and diameter were averaged over three

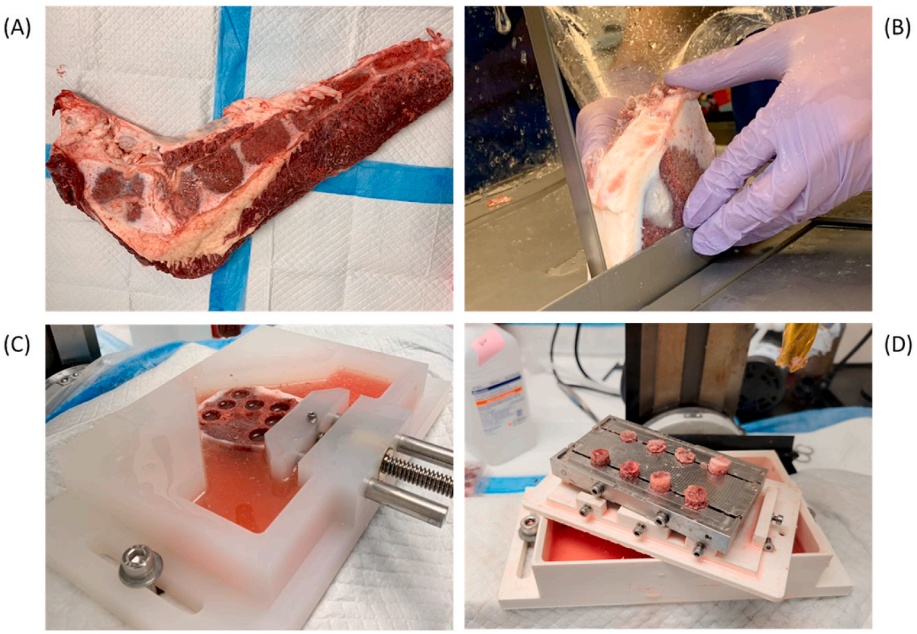

Fig. 1. (A) 18-month-old bovine sternum. (B) Slicing process of the segmented bovine sternum with the Exakt 312 diamond-coated pathology saw. (C) Polypropylene coring clamp with a cored sternum slice, fixed to the vertical mill for bone core fabrication. (D) ABS holder and insert with the stainless-steel mill clamp and eight bone cores during the bone core milling process.

repeat measurements with a vernier caliper (±0.02 mm). Of the 40 bone cores prepared, the 23 viable bone cores that best met dimensional requirements (10 mm × 10 mm) with minimal visible edge and surface artefacts and damage were selected for this study.

2.3. Bone core ex vivo culture

Following the 4-day recovery period, each bone core was placed in a sterile MED610^{TM} bioreactor between two sapphire pistons and assembled with a sterile medium reservoir and tubing circuit (Fig. 2). All bone cores were assembled in bioreactors within 48 h following the 4-day recovery period. Bone cores were maintained in the bioreactors for 21-days at 37 °C and 5% CO_2 with constant culture medium (DMEM/F-12 supplemented with 10% FBS, 1% AA, and 10 μg/mL of L-ascorbic acid 2-phosphate) at 6.6 mL/h (Meyer et al., 2016; Vivanco et al., 2013) using two 24-channel peristaltic pumps (Ismatec^{TM} ISM939D, No. 7800041, Cole-Parmer Canada, Montreal, QB, Canada). Each reservoir contained 6 mL of medium that was changed three times a week. Throughout the study, medium pH was monitored via pH strips on medium change days with no significant differences observed across the control and treatment groups. Additionally, no visible signs of contamination were observed in medium reservoirs or bone core samples.

2.4. Mechanical load treatment

Twenty-four hours post-bioreactor assembly, bone cores were ranked from lowest to highest E_{app}. Bone cores were divided based on their rank into two groups with equal mean E_{app}, a no-load control group (n = 11) and a load treatment group (n = 12). E_{app} ranks were acquired via quasi-static compression loading on day 0 with a 10 N preload followed by an applied strain of −4000 με at a rate of 50 με/s. Additional tests were performed on days 8 and 21 to assess the change in E_{app}. Load group bone cores were stimulated 5-days a week for 21-days with cyclic loading, which consisted of a 10 N preload followed by a sinusoidal load with a maximum change in applied strain of 4000 με (−1000 to −5000 με) for 120 cycles at 2 Hz (Meyer et al., 2016). For all tests, displacement was controlled, corrected for system compliance (García-Rodríguez et al., 2008) and normalized to individual core height to minimize applied strain variance. During all loading, bone cores were loaded in random order at room temperature with a Mach-1 mechanical loading system (Biomomentum, Laval, QB, Canada) and a lubricated

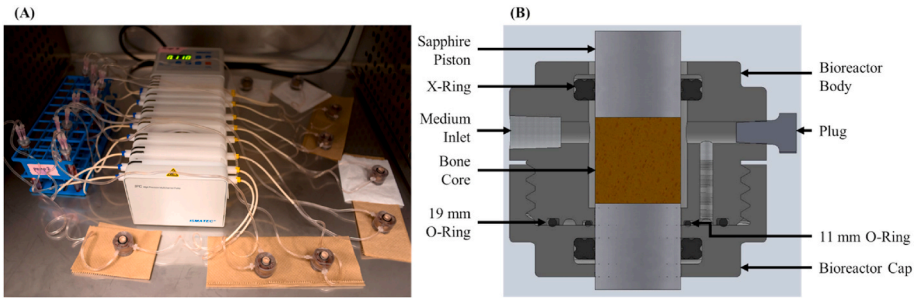

Fig. 2. (A) MED610^{TM} bioreactors containing trabecular bone cores with continuous culture medium perfusion. Media reservoirs, peristaltic pump, tubing, and luers were adapted from Vivanco et al. (2013) and Meyer et al. (2016). (B) Section view of the MED610^{TM} bioreactor chamber with a representative bone core, tapered MED610^{TM} plug seal, sapphire pistons, and silicone rubber O-ring and X-ring seals. Bioreactor chamber changes from previous studies (Vivanco et al., 2013; Meyer et al., 2016) included material (MED610^{TM}), increased alcove height for up to 11 mm tall samples, and minor adjustments for 3D printing fabrication including support material removal.

ball-and-socket fixture (Fig. 3). Loading conditions were performed at room temperature and not at simulated physiological conditions (37 °C and 5% CO_2) due to loading system and incubator restrictions.

Time, force, and displacement were recorded with a multiple-axis 250 N (±0.0065 N) load cell (MA242, Biomomentum) and analyzed in MATLAB 2019b (MathWorks, Natick, MA, USA). Strain (ε) and E_{app} were calculated by assuming Hooke's law (Equation (1)) with the last 50% of the linear force-displacement curve (Fig. 4; $R^2_{avg} > 0.99$); where F represents force (N), H is the sample bone core height (mm), δ is the axial displacement due to compression (mm), and A_c is the bone core cross-sectional area (mm^2). All E_{app} calculations were made assuming initial bulk dimensions.

$$E_{app} = \frac{FH}{\delta A_c}, \varepsilon = \frac{\delta}{H} \tag{1}$$

The percent change of E_{app} (%ΔE_{app}) was calculated between days 0, 8, and 21 using Equation (2), where the subscripts indicate the days compared.

$$\%\Delta E_{app} = \left(\frac{E_{app,day\ Y} - E_{app,day\ X}}{E_{app,day\ X}}\right) \times 100\% \tag{2}$$

2.5. Statistical analysis

All statistical analyses were performed in MATLAB 2019b and Origin 2021b (OriginLab Corporation, Northampton, MA, USA) and assumed a significance level of 5% ($\alpha = 0.05$). Results are presented as the mean ± the standard deviation. Mean E_{app} differences between the Load and control groups were compared with percentage differences. Group normality was evaluated with Shapiro-Wilk tests and confirmed a lack of normality across all groups. A Wilcoxon rank-sum test was applied to assess E_{app} significance between the Load and control group for all 23 bone cores and ensure that the groups were comparable on day 0. All other analyses excluded the six bone cores removed after day 8 (Load group: n = 9; control group: n = 8). The statistical significance between the Load and control group E_{app} was assessed with Wilcoxon tests on days 0, 8, and 21. Additional Wilcoxon tests were performed to analyze the difference in %ΔE_{app} between the Load and control groups for days 0–8, 0–21, and 8–21 and evaluate the effect of mechanical loading on trabecular bone stiffness. The statistical significance of E_{app} and %ΔE_{app} within each group were evaluated with Friedman's non-parametric repeated measures analysis of variance (ANOVA) and Dunn's multiple comparison post hoc test. Based on test results from the current study, the minimum required sample size was calculated for an assumed 80% probability of type II error and nonparametric distribution.

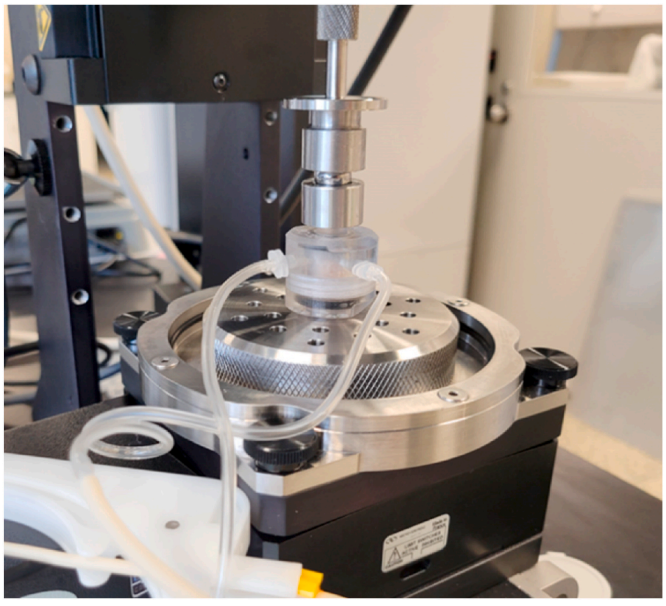

Fig. 3. MED610™ bioreactor and fixture assembly with the Mach-1 mechanical loading system. Bone cores were tested and stimulated at room temperature but remained assembled in their closed-loop bioreactor systems with culture medium.

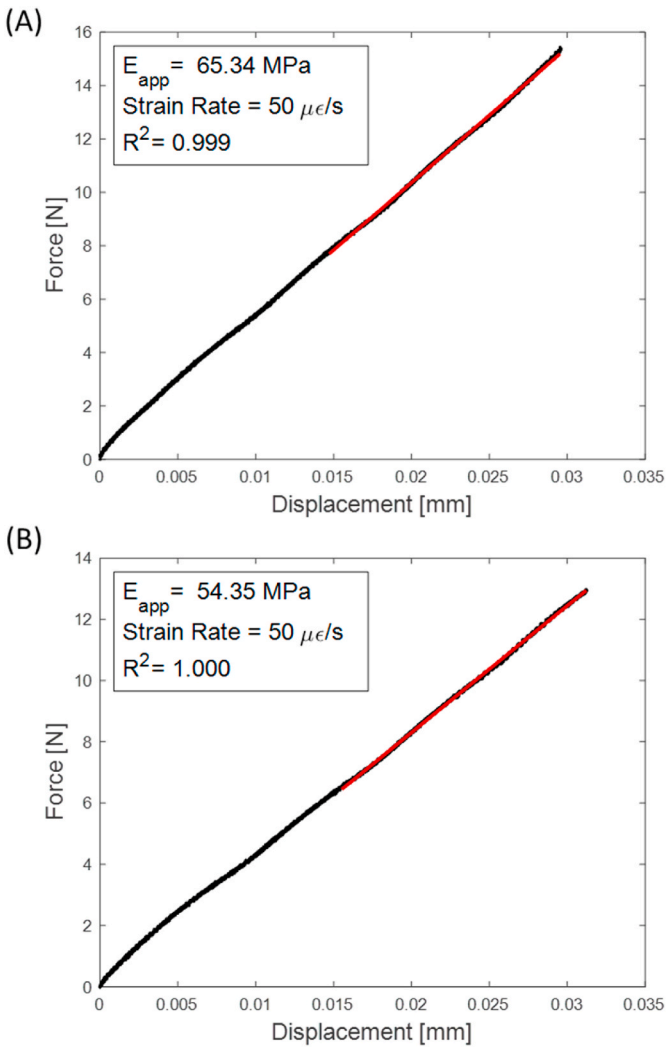

Fig. 4. Sample representative force-displacement plots from quasi-static loading of bovine trabecular bone cores for the (A) control (H = 9.83 ± 0.02 mm; A_c = 75.3 ± 0.04 mm) and (B) Load (H = 9.78 ± 0.04 mm; A_c = 74.5 ± 0.16 mm) groups on day 0 of the study. The linear fit shown (red) was performed with the last 50% of the force-displacement curve and demonstrates the apparent bone core stiffness used to determine the apparent elastic modulus of bone cores.

3. Results

The mean and standard deviation E_{app} for all 23 bone cores on day

Table 1
Mean core dimensions (± standard deviation (SD)) observed for the Load and control groups on day 0.

Treatment Group	Height [mm]	Diameter [mm]
	Day 0	Day 0
Load (n = 9)	9.80 (±0.235)	9.77 (±0.113)
Control (n = 8)	9.91 (±0.0950)	9.83 (±0.0290)
Percentage Difference	1.13%	0.64%

0 was 56.4 ± 16.4 MPa. The core dimensions and E_{app} were not statistically different between experiment groups on day 0 (Table 1).

After day 8, three bone cores were discarded from each group due to continuous bioreactor leakage causing them to dry out and therefore, were not included in the E_{app} results presented. Fig. 5 displays the E_{app} values computed for the Load and control groups on days 0, 8, and 21. Friedman's non-parametric repeated measures ANOVA showed that the E_{app} was statistically significant across the time points for the Load ($p = 0.003$) and control groups ($p = 0.008$). For the Load group, the day 0 E_{app} was statistically significant from day 21 ($p = 0.003$) but days 0 and 8 ($p = 0.055$) and days 8 and 21 ($p = 1.00$) were not significantly different. The control group E_{app} was not statistically significant between days 0 and 8 ($p = 1.00$) and days 0 and 21 (0.073), though days 8 and 21 were significantly different ($p = 0.008$). E_{app} was not statistically significant between the Load and control groups on day 0 ($p = 0.815$), day 8 ($p = 0.059$), and day 21 ($p = 0.277$). Although the Load and control E_{app} had no statistical differences, the Load group E_{app} values were 6.88%, 46.1%, and 32.9% higher for days 0, 8, and 21, respectively. Overall, a higher percent change in the Load versus control group E_{app} was observed.

Friedman ANOVA tests showed that within the Load and control groups, the $\%\Delta E_{app}$ for all day comparisons were significantly different (Load: $p = 0.002$; control: $p = 0.010$, Fig. 6). For the Load group, the day 0–21 $\%\Delta E_{app}$ (53.4 ± 41.4%) was statistically different ($p = 0.001$) from day 8–21 (4.04 ± 17.4%), but was not different from day 0–8 (46.5 ± 30.3%, $p = 0.472$), while days 0–8 and 8–21 were not significantly different ($p = 0.102$). For the control group $\%\Delta E_{app}$, day 0–8 (0.0329 ± 8.40%) was statistically significant from days 0–21 (20.9 ± 18.4%, $p = 0.037$) and 8–21 (20.7 ± 13.3%, $p = 0.018$).

Wilcoxon tests found that the Load and control $\%\Delta E_{app}$ values were statistically significant for day 0–8 ($p < 0.001$) but not for day 8–21 ($p = 0.059$). Although the $\%\Delta E_{app}$ for the Load group was not statistically significant from the control for day 0–21 ($p = 0.059$), it was more than twice as large (53.4% versus 20.9%).

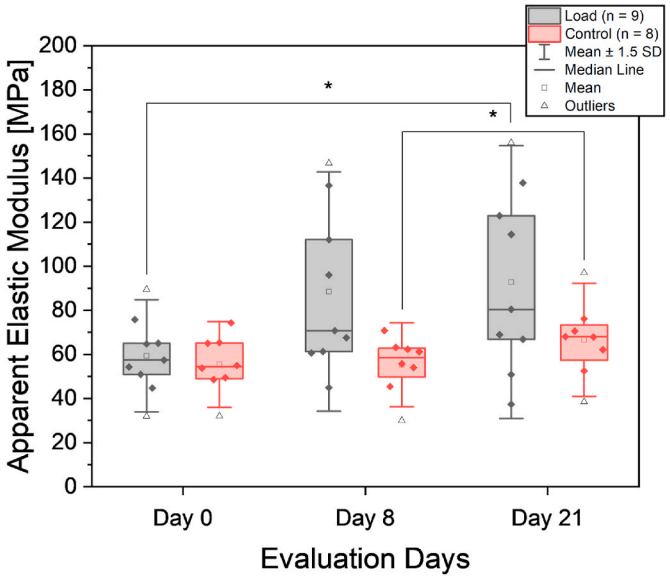

Fig. 5. Measured apparent elastic modulus evaluated for load treated and control bone core groups on days 0, 8, and 21 (*$p < 0.05$). Load group mean E_{app} for days 0, 8, and 21 were 59.4 ± 17.0, 88.5 ± 36.2, and 92.8 ± 41.3 MPa, mean ± SD, respectively. Control group mean E_{app} for days 0, 8, and 21 were 55.4 ± 13.0, 55.4 ± 12.7, and 66.6 ± 17.1 MPa, mean ± SD, respectively. The Load group day 21 E_{app} was 44.5% higher than day 0; and control group day 21 E_{app} was 19.0% higher than day 0.

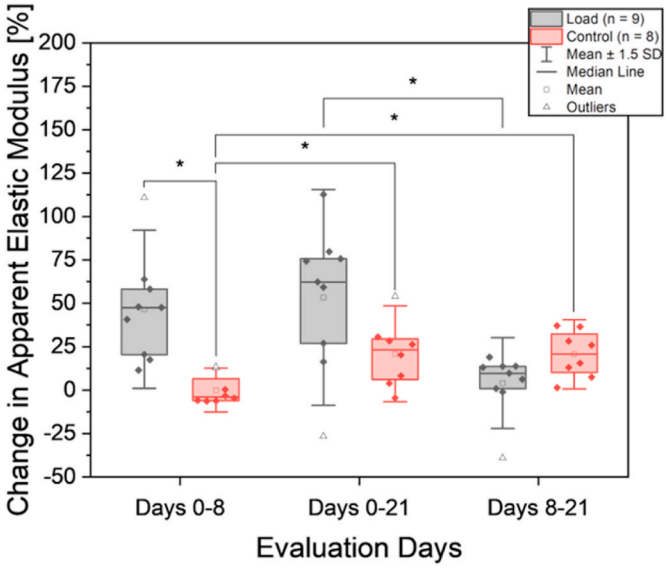

Fig. 6. Percent change in apparent elastic modulus ($\%\Delta E_{app}$) between days 0 and 8, 0 and 21, and 8 and 21 for the Load and control groups (*$p < 0.05$).

4. Discussion

In this study, an initial E_{app} range of 28.6–89.5 MPa was observed across all 23 bone cores with a mean of 56.4 ± 16.4 MPa, which is comparable to previous results found by Vivanco et al. (2013) for 10 mm diameter by 5 mm high bovine sternum trabecular bone cores (treatment: 50.77 ± 11.85 MPa (± standard error of mean (SEM)), control: 30.09 ± 7.70 MPa (±SEM)). However, the day 0 average E_{app} observed is comparably less (~83% less) than the day 1 average (136 ± 12.8 MPa (± standard error)) found by Meyer et al. (2016). Though these studies also tested bovine sternum trabecular bone, variance in E_{app} should be expected across different animals due to the anisotropic and heterogeneous nature of trabecular bone as well as the age and health of the animal (Carretta et al., 2013; Oftadeh et al., 2015). Variability across sample trabecular structure could have masked significant differences between the Load and control groups E_{app} despite the Load group having average E_{app} values 46.1% and 32.9% higher on days 8 and 21, respectively, compared to the control.

Although the Load group E_{app} was not significantly different from the control, the Load group had a much higher (46.5% versus 0.0329%) change in E_{app} between days 0 and 8 and a lower (4.04% versus 20.7%) change between days 8 and 21. Though the E_{app} changes were not statistically significant, load and bone formation relationships found in previous studies (Meyer et al., 2016; Mann et al., 2006) suggest that the loaded bone cores experienced more bone formation within the first eight days of the experiment, while the non-loaded bone cores experienced more bone formation over the last 13 days. Vivanco et al. (2013) observed a similar trend in which they found that the E_{app} of bovine trabecular bone loaded daily with a maximum strain of −4000 με increased by 38% more within the first seven days compared to the last 11 days of the study. Additionally, Vivanco et al. (2013) found that a non-loaded control group had a 14% higher E_{app} change within the first seven days compared to the following 11 days, whereas this study found that the control group $\%\Delta E_{app}$ was 20.7% higher during the last 13 days compared to the first eight days. Trabecular bone has a rapid bone formation healing process in response to injury with woven bone mineralization and osteoid formation shown to form within 1–2 weeks for small animals and humans (Sandberg and Aspenberg, 2016). Therefore, it is possible that the Load group E_{app} increase over the first eight days occurred due to osteoid formation in response to injuries sustained during bone core preparation. Meyer et al. (2016) found that

prostaglandin E2 (PGE2) concentrations in a non-loaded control group were elevated and similar to bone cores treated with mechanical load (maximum change of −2000 με) after eight days but decreased after day 12 and were significantly different from the treatment groups by day 15. PGE2 levels are vital to bone formation during injury response, with elevated levels increasing bone mineral content and strength (Li et al., 2007). Thus, one would have expected that the Load group E_{app} would have continued to increase after day 8 in response to the mechanical loading. The current study implemented daily cyclic loading with a max strain of −5000 με, which may have caused bone fatigue or damage over time and attributed to the minimal E_{app} increase between days 8 and 21. The elevated PGE2 levels observed by Meyer et al. (2016) suggest that an increase in the control group E_{app} would have been expected before day 8 in response to injuries sustained during core preparation.

Overall, the Load group $\%\Delta E_{app}$ over 21-days was not significantly different from the control group but increased by more than twice (53.4% versus 20.9%) the control. Any significant difference between the Load and control group $\%\Delta E_{app}$ could have been masked by type II statistical error due to the large variance in the Load group E_{app}. A statistical power analysis suggests at least twelve specimens per group were required to achieve 80% power. Three bone cores were discarded from each group due to bioreactor leakage. An improved bioreactor design will be implemented for future experiments. Despite this, the results suggest that an adequate amount of viable bone cells were present to promote bone adaptation during the 21-day culture. However, it is unclear if the MED610^{TM} material affected bone cell behaviour and the bone adaptation process. Ngan et al. (2019) demonstrated in 2D and 3D *in vitro* cultures that MED610^{TM} did not inhibit cell viability and differentiation after 10-days. Furthermore, Ngan et al. (2019) found that MED610^{TM} did not produce a significant foreign-body response when implanted *in vivo* for 2-weeks. To confirm the role of MED610^{TM} in the 3D printed bioreactor during direct contact with trabecular bone, additional studies should be performed with histological analyses to measure bone mineral apposition and cell apoptosis rates.

This study had several limitations. The sample size of each group was small and had considerable variance, specifically in the Load group, which made it difficult to confirm the normality of individual data sets. Choosing a non-parametric analysis for all comparisons may have increased the type II statistical error in group comparisons. Care was taken in sample preparation to minimize variance in core dimensions and applied strain levels. Additional possible sources of error include bone structure variability (Carretta et al., 2013; Oftadeh et al., 2015), end and side artefacts (Bennison et al., 2021; Keaveny et al., 1997; Lievers et al., 2010), and bone cell apoptosis. E_{app} is dependent on the anisotropic and heterogeneous orientation of the trabecular structure which varies throughout the tissue (Bennison et al., 2020; Carretta et al., 2013; Oftadeh et al., 2015). Inconsistent sample trabecular orientation alignment with the loading direction may have increased variability during compression loading. Side and end artefacts that form during bone core extraction from trabecular tissue cause inaccurate estimations of E_{app} during mechanical loading (Bennison et al., 2021). 10 mm diameter bone cores with an aspect ratio of 1 were prepared for this study to ensure sample dimensions were adequate for continuum assumptions (Keaveny et al., 1997; Lievers et al., 2010), prevent sample buckling (Zhao et al., 2018), and minimize side artefact effects (Lievers et al., 2010). Additionally, a ball-and-socket fixture was implemented to minimize the effect of unparallel surfaces during loading. Inaccuracies due to end artefacts are assumed to have been minimized since small "toe" regions were consistently observed in sample force-displacement curves (Fig. 4) (Meyer et al., 2016). Previous studies have confirmed culture medium diffusion and minimal cell apoptosis throughout 5 mm × 10 mm (H x D) trabecular bone cores during long-term culture (Davies et al., 2006; Mann et al., 2006). Although the bone core height was increased to 10 mm for this study to meet bone mechanical testing recommendations (Zhao et al., 2018), it is unclear if the increased height limited medium diffusion to the centre of bone cores. A lack of medium diffusion could have reduced cell viability and bone hydration and caused apparent stiffness overestimates (Wescott, 2019). Lastly, bone core relaxation was observed during the controlled cyclic loads. Trabecular bone has time-dependent (viscoelastic) behaviour (Lakes, 2009; Wescott, 2019). As a result, trabecular bone relaxes and has strain rate-dependent mechanical properties during mechanical loading, which could affect the accuracy of tissue loading applications.

Despite these limitations, this study demonstrated that an *ex vivo* bovine trabecular bone experiment with a 3D printed MED610^{TM} bioreactor design could replicate E_{app} trends over 21-days in mechanically loaded bone cores found by Vivanco et al. (2013). However, future studies with a larger sample size and histological analyses are warranted to reduce the variability of measured mechanical behaviour within groups and assess cell viability and bone mineral apposition throughout organ culture.

CRediT authorship contribution statement

Brian A. Kunath: Writing – review & editing, Writing – original draft, Visualization, Methodology, Investigation, Formal analysis. **Kail Beloglowka:** Writing – review & editing, Methodology, Investigation, Formal analysis. **Roshni Rainbow:** Writing – review & editing, Supervision, Funding acquisition, Conceptualization. **Heidi-Lynn Ploeg:** Writing – review & editing, Supervision, Funding acquisition, Conceptualization.

Declaration of competing interest

The authors declare that they have no known competing financial interests or personal relationships that could have appeared to influence the work reported in this paper.

Data availability

Data will be made available on request.

Acknowledgments

We acknowledge the support of the Natural Sciences and Engineering Research Council of Canada/le Conseil de recherches en sciences naturelles et en genie du Canada (NSERC/CRSNG), [RGPAS/00128–2019, RGPIN/07210-2019, RGPIN-2019-04906, and DGECR-2019-00363], the Canadian Foundation for Innovation/Fondation Canadienne pour l'Innovation John R. Evans Leaders Fund (CFI/FCI JELF), CONNECT! NSERCE CREATE grant, the Ontario Graduate Scholarship program, the Queen's University Faculty of Engineering and Applied Science, and the Centre for Health Innovation, Queen's University, Kingston, ON, Canada.

References

Bellido, T., Delgado-Calle, J., 2020. Ex vivo organ cultures as models to study bone biology. J. Bone Miner. Res. 4.
Bennison, M.B.L., Pilkey, A.K., Lievers, W.B., 2020. Misalignment error in cancellous bone apparent elastic modulus depends on bone volume fraction and degree of anisotropy. J. Biomech. Eng. 143.
Bennison, M.B.L., Pilkey, A.K., Lievers, W.B., 2021. Evaluating a theoretical and an empirical model of "side effects" in cancellous bone. Med. Eng. Phys. 94, 8–15.
Canadian Chronic Disease Surveillance System, 2021. Osteoporosis and Related Fractures in Canada. Public Health Agency of Canada, Ottawa, ON.
Carretta, R., Lorenzetti, S., Müller, R., 2013. Towards patient-specific material modeling of trabecular bone post-yield behavior. Int. J. Num. Meth. Biomed. Eng. 29, 250–272.
Clynes, M.A., Harvey, N.C., Curtis, E.M., Fuggle, N.R., Dennison, E.M., Cooper, C., 2020. The epidemiology of osteoporosis. Br. Med. Bull. 133, 105–117.
Cramer, E.E.A., Ito, K., Hofmann, S., 2021. Ex vivo bone models and their potential in preclinical evaluation. Curr. Osteoporos. Rep. 19, 75–87.
Currens, E.R., Armbruster, M.R., Castiaux, A.D., Edwards, J.L., Martin, R.S., 2022. Evaluation and optimization of PolyJet 3D-printed materials for cell culture studies. Anal. Bioanal. Chem. 414, 3329–3339.

Currey, J.D., 2012. The structure and mechanics of bone. J. Mater. Sci. 47, 41–54.
David, V., Guignandon, A., Martin, A., Malaval, L., Lafage-Proust, M.-H., Rattner, A., Mann, V., Noble, B., Jones, D.B., Vico, L., 2008. Ex vivo bone formation in bovine trabecular bone cultured in a dynamic 3D bioreactor is enhanced by compressive mechanical strain. Tissue Eng. 14, 117–126.
Davies, C.M., Jones, D.B., Stoddart, M.J., Koller, K., Smith, E., Archer, C.W., Richards, R. G., 2006. Mechanically loaded ex vivo bone culture system 'Zetos': systems and culture preparation. Eur. Cell. Mater. 11, 57–75.
Endres, S., Kratz, M., Wunsch, S., Jones, D., 2009. Zetos: a culture loading system for trabecular bone. Investigation of different loading signal intensities on bovine bone cylinders. J. Musculoskelet. Neuronal Interact. 9, 173–183.
Frost, H.M., 1987. Bone "mass" and the "mechanostat": a proposal. Anat. Rec. 219, 1–9.
Frost, H.M., 2003. Bone's mechanostat: a 2003 update. Anat. Rec. A Discov. Mol. Cell. Evol. Biol. 275, 1081–1101.
García-Rodríguez, S., Smith, E.L., Ploeg, H.-L., 2008. A calibration procedure for a bone loading system. J. Med. Dev. Trans. ASME 2, 011006.
Heuer, C., Preuß, J.-A., Habib, T., Enders, A., Bahnemann, J., 2021. 3D printing in biotechnology—an insight into miniaturized and microfluidic systems for applications from cell culture to bioanalytics. Eng. Life Sci. 1–16.
Keaveny, T.M., Pinilla, T.P., Crawford, R.P., Kopperdahl, D.L., Lou, A., 1997. Systematic and random errors in compression testing of trabecular bone. J. Orthop. Res. 15, 101–110.
Kendler, D.L., Adachi, J.D., Brown, J.P., Juby, A.G., Kovacs, C.S., Duperrouzel, C., McTavish, R.K., Cameron, C., Slatkovska, L., Burke, N., 2021. A scorecard for osteoporosis in Canada and seven Canadian provinces. Osteoporos. Int. 32, 123–132.
Kreß, S., Schaller-Ammann, R., Feiel, J., Priedl, J., Kasper, C., Egger, D., 2020. 3D printing of cell culture devices: assessment and prevention of the cytotoxicity of photopolymers for stereolithography. Materials 13, 3011.
Lakes, R.S., 2009. Viscoelastic Materials. Cambridge University Press, New York.
Li, M., Thompson, D.D., Paralkar, V.M., 2007. Prostaglandin E(2) receptors in bone formation. Int. Orthop. 31, 767–772.
Lievers, W.B., Petryshyn, A.C., Poljsak, A.S., Waldman, S.D., Pilkey, A.K., 2010. Specimen diameter and "side artifacts" in cancellous bone evaluated using end-constrained elastic tension. Bone 47, 371–377.
Little-Letsinger, S.E., Rubin, J., Diekman, B., Rubin, C.T., McGrath, C., Pagnotti, G.M., Klett, E.L., Styner, M., 2022. Exercise to mend aged-tissue crosstalk in bone targeting osteoporosis & osteoarthritis. Semin. Cell Dev. Biol. 123, 22–35.
Mann, V., Huber, C., Kogianni, G., Jones, D., Noble, B., 2006. The influence of mechanical stimulation on osteocyte apoptosis and bone viability in human trabecular bone. J. Musculoskelet. Neuronal Interact. 6, 408–417.
Marino, S., Staines, K.A., Brown, G., Howard-Jones, R.A., Adamczyk, M., 2016. Models of ex vivo explant cultures: applications in bone research. BoneKEy Rep. 5, 818-818.
Martin, R.B., Burr, D.B., Sharkey, N.A., 1998. Skeletal Tissue Mechanics. Springer-Verlag, New York.
McMillan, L.B., Zengin, A., Ebeling, P.R., Scott, D., 2017. Prescribing physical activity for the prevention and treatment of osteoporosis in older adults. Healthcare 5, 85.
Meyer, L.A., Johnson, M.G., Cullen, D.M., Vivanco, J.F., Blank, R.D., Ploeg, H.L., Smith, E.L., 2016. Combined exposure to big endothelin-1 and mechanical loading in bovine sternal cores promotes osteogenesis. Bone 85, 115–122.
Mustahsan, V.M., Anugu, A., Komatsu, D.E., Kao, I., Pentyala, S., 2021. Biocompatible customized 3D bone scaffolds treated with CRFP, an osteogenic peptide. Bioengineering 8, 199.
Ngan, C.G.Y., O'Connell, C.D., Blanchard, R., Boyd-Moss, M., Williams, R.J., Bourke, J., Quigley, A., McKelvie, P., Kapsa, R.M.I., Choong, P.F.M., 2019. Optimising the biocompatibility of 3D printed photopolymer constructs in vitro and in vivo. Biomed. Mater. 14, 035007.
Oftadeh, R., Perez-Viloria, M., Villa-Camacho, J.C., Vaziri, A., Nazarian, A., 2015. Biomechanics and mechanobiology of trabecular bone: a review. J. Biomech. Eng. 137, 0108021-01080215.
Ozcivici, E., Luu, Y.K., Rubin, C.T., Judex, S., 2010. Low-level vibrations retain bone marrow's osteogenic potential and augment recovery of trabecular bone during reambulation. Publ. Libr. Sci. One 5, e11178.
Priyadarshini, B.M., Dikshit, V., Zhang, Y., 2020. 3D-printed bioreactors for in vitro modeling and analysis. Int. J. Bioprint. 6, 267.
Rosa, N., Simoes, R., Magalhaes, F.D., Marques, A.T., 2015. From mechanical stimulus to bone formation: a review. Med. Eng. Phys. 37, 719–728.
Sandberg, O.H., Aspenberg, P., 2016. Inter-trabecular bone formation: a specific mechanism for healing of cancellous bone. Acta Orthop. 87, 459–465.
Stratasys, 2018. MED610™ Biocompatibility Requirements. Printing Biocompatible Parts on PolyJet™ 3D Printers with MED610™, DOC-08381 Rev. F ed. Stratasys, Eden Prairie, pp. 1–5.
Su, X., Wang, T., Guo, S., 2021. Applications of 3D printed bone tissue engineering scaffolds in the stem cell field. Regener. Ther. 16, 63–72.
Tong, X., Chen, X., Zhang, S., Huang, M., Shen, X., Xu, J., Zou, J., 2019. The effect of exercise on the prevention of osteoporosis and bone angiogenesis. BioMed Res. Int. 8, 2019.
Vivanco, J., Garcia, S., Ploeg, H.L., Alvarez, G., Cullen, D., Smith, E.L., 2013. Apparent elastic modulus of ex vivo trabecular bovine bone increases with dynamic loading. Proc. IME H J. Eng. Med. 227, 904–912.
Wescott, D.J., 2019. Postmortem change in bone biomechanical properties: loss of plasticity. Forensic Sci. Int. 300, 164–169.
Zhao, S., Arnold, M., Ma, S., Abel, R.L., Cobb, J.P., Hansen, U., Boughton, O., 2018. Standardizing compression testing for measuring the stiffness of human bone. Bone & Joint Res. 7, 524–538.